

IMPACT CRATERING

The surfaces of most solid planets and moons in the solar system are scarred with circular craters produced by the impacts of smaller objects. More than 100 impact craters ranging in size from tens of meters to 140 km have also been recognized on Earth. Fresh impact craters are roughly circular rimmed depressions surrounded by hummocky blankets of debris. They form when an extraterrestrial body strikes the Earth or other planet at a velocity exceeding a few km/sec. Crater formation is an orderly, although rapid, process that begins when the impacting body first strikes the planet's surface and ends after the debris around and within the crater comes to rest. The crater is excavated by strong shock waves created as the impacting body plunges into the surface. These shock waves also cause diagnostic high-pressure mineralogical changes in the rocks surrounding the crater. The size of the final crater is a function of the speed and mass of the projectile that created it, as well as such other factors as the angle of impact and acceleration of gravity. Impact cratering is the dominant process sculpting the surfaces of asteroids and small satellites. Cratering also played a major role in the growth of all of the planets: it is now believed that impacts between planetary embryos and objects of perhaps 10% of their mass dominated every stage of the first 100 Myr of solar system history. A later era of heavy bombardment created the ancient cratered terranes on the Moon, Mercury and Mars between 4.5 and about 3.2 Gyr ago. The Earth's early Archean history was probably strongly affected by large impacts. In the subsequent history of the Earth, a large impact caused at least one major biological extinction at the end of the Cretaceous era.

History of Investigation

Craters were discovered in 1610 when Galileo pointed his first crude telescope at the Moon. Galileo recognized their raised rims and central peaks, but described them only as circular "spots" on the moon. Although Galileo himself did not record an opinion on how they formed, astronomers argued about their origin for the next three centuries. The word "crater" was first used in a non-genetic sense by the astronomer J. H. Schröter in 1791. Until the 1930's most astronomers believed the Moon's craters were giant extinct volcanoes: the impact hypothesis, proposed sporadically over the centuries, did not gain a foothold until improving knowledge of impact physics showed that even a moderately oblique high-speed impact produces a circular crater rather than an elliptical crater, consistent with the observed circularity of nearly all of the Moon's craters. Even so, many astronomers clung to the volcanic theory until the high resolution imagery and

direct investigation of the Apollo program in the early 1970's firmly settled the issue in favor of an impact origin for nearly all lunar craters. In the current era spacecraft have initiated the remote study of impact craters on other planets, beginning with Mariner IV's unexpected discovery of craters on Mars on July 15, 1965. Since then craters have been found on almost every other solid body in the solar system.

The first terrestrial structure shown unambiguously to be created by a large impact was Meteor Crater, Arizona. This 1 km diameter crater and its associated meteoritic iron was investigated in detail by D. M. Barringer from 1906 until his death in 1929. After Barringer's work a large number of small impact structures resembling Meteor Crater have been found. Impact structures larger than about 5 km in diameter were first described as "cryptovolcanic" because they showed signs of violent upheaval but were not associated with the eruption of volcanic materials. J. D. Boon and C. C. Albritton in 1937 proposed that these structures were really caused by impacts, although final proof had to wait until the 1960's when the presence of the shock-metamorphic minerals coesite and stishovite proved that the Ries Kessel in Germany was the result of a large meteor impact.

Theoretical and experimental work on the mechanics of cratering began during World War II and was extensively developed in later years. This work was spurred partly by the need to understand the craters produced by nuclear weapons and partly by the fear that the "meteoroid hazard" to space vehicles would be a major barrier to space exploration. Computer studies of impact craters were begun in the early 1960's. A vigorous and highly successful experimental program to study the physics of impact was initiated by D. E. Gault at NASA's Ames facility in 1965.

These three traditional areas of astronomical crater studies, geological investigation of terrestrial craters, and the physics of cratering have blended together in the post-Apollo era. Traditional boundaries have become blurred as extraterrestrial craters are subjected to direct geologic investigation, the Earth's surface is scanned for craters using satellite images, and increasingly powerful computers are used to simulate the formation of both terrestrial and planetary craters on all size scales. The recent proposals that the Moon was created by the impact of a Mars-size protoplanet with the proto-Earth 4.5 Gyr ago and that the Cretaceous era was ended by the impact of a 10 km diameter asteroid or comet indicate that the subject of impact cratering is far from exhausted and that new results may be expected in the future.

Crater Morphology

Fresh impact craters can be grossly characterized as "circular rimmed depressions". Although this description can be applied to all craters, independent of size, the detailed form of craters varies with size, substrate material, planet, and age. Craters have been observed over a range of sizes varying from 0.1 μm (microcraters first observed on lunar rocks brought back by the Apollo astronauts) to the more than 2000 km diameter Hellas basin on Mars. Within this range a common progression of morphologic features with increasing size has been established, although exceptions and special cases are not uncommon.

Simple Craters. The classic type of crater is the elegant bowl-shaped form known as a "simple crater" (Fig. 1a). This type of crater is common at sizes less than about 15 km diameter on the moon and 3 to about 6 km on the Earth, depending on the substrate rock type. The interior of the crater has a smoothly-sloping parabolic profile and its rim-to-floor depth is about 1/5 of its rim-to-rim diameter. The sharp-crested rim stands about 4% of the crater diameter above the surrounding plain, which is blanketed with a mixture of ejecta and debris scoured from the preexisting surface for a distance of about one crater diameter from the rim. The thickness of the ejecta falls off as roughly the inverse cube of distance from the rim. The surface of the ejecta blanket is characteristically hummocky, with mounds and hollows alternating in no discernible pattern. Particularly fresh simple craters may be surrounded by fields of small secondary craters and bright rays of highly pulverized ejecta that extend many crater diameters away from the primary. Meteor Crater, Arizona, is a slightly eroded representative of this class of relatively small craters. The floor of simple craters is underlain by a lens of broken rock, "breccia", which slid down the inner walls of the crater shortly following excavation. This breccia typically includes representatives from all of the formations intersected by the crater and may contain horizons of melted or highly shocked rock. The thickness of this breccia lens is typically 1/2 to 1/3 of the rim-to-floor depth.

Complex Craters. Lunar craters larger than about 20 km diameter and terrestrial craters larger than about 3 km have terraced walls, central peaks, and at larger sizes may have flat interior floors or internal rings instead of central peaks. These craters are believed to have formed by collapse of an initially bowl-shaped "transient crater", and because of this more complicated structure are known as "complex craters" (Fig. 1b). The transition between simple and complex craters has now been observed on the Moon, Mars, Mercury and the Earth, as well as on some of the icy satellites in the outer solar system. In general the transition diameter scales as g^{-1} , where g is the acceleration of gravity at the planet's surface, although the constant in the scaling rule is not the same for

icy and rocky bodies. This is consistent with the idea that complex craters form by collapse, with icy bodies having only about 1/3 the strength of rock ones. The floors of complex craters are covered by melted and highly shocked debris, and melt pools are sometimes seen in depressions in the surrounding ejecta blanket. The surfaces of the terrace blocks tilt outward into the crater walls, and melt pools are also common in the depressions thus formed. The most notable structural feature of complex craters is the uplift beneath their centers. The central peaks contain material that is pushed upward from the deepest levels excavated by the crater. Study of terrestrial craters has shown that the amount of structural uplift h_{SU} is related to the final crater diameter D by

$$h_{SU} = 0.06D^{1.1}$$

where all distances are in kilometers. The diameter of the central peak complex is roughly 22% of the final rim-to-rim crater diameter in craters on all the terrestrial planets.

Complex craters are generally shallower than simple craters of equal size and their depth increases slowly with increasing crater diameter. On the Moon, the depth of complex craters increases from about 3 km to only 6 km while crater diameter ranges from 20 to 400 km. Rim height also increases rather slowly with increasing diameter because much of the original rim slides into the crater bowl as the wall collapses. Complex craters are thus considerably larger than the transient crater from which they form: estimates suggest that the crater diameter may increase as much as 60% during collapse.

As crater size increases the central peaks characteristic of smaller complex craters give way to a ring of mountains (Fig. 1c). This transition takes place at about 140 km diameter on the Moon, 75 km on Mercury, 45 km on Mars and about 20 km on the Earth, again following a g^{-1} rule. The diameter of the central ring is generally about 0.5 of the rim-to-rim diameter of the crater on all the terrestrial planets.

The ejecta blankets of complex craters are generally similar to those of simple craters, although the "hummocky" texture characteristic of simple craters is replaced by more radial troughs and ridges as size increases. Fresh complex craters also have well developed fields of secondary craters, including frequent clusters and "herringbone" chains of closely associated, irregular secondary craters. Martian and Venusian craters have flow-textured ejecta blankets that suggest fluidization by water or atmospheric gasses. Very fresh craters, such as Copernicus and Tycho on the Moon, have far-flung bright ray systems whose nature is not well understood.

Multiring Basins. The very largest impact structures are characterized by multiple concentric circular scarps, and are hence known as "multiring basins". The most famous such structure is the 930 km diameter Orientale basin on the Moon (Fig. 1d),

which has at least 4 nearly complete rings of inward-facing scarps. Although opinion on the origin of the rings still varies, most investigators feel that the scarps represent circular normal faults that slipped shortly after the crater was excavated. There is little doubt that multiring basins are caused by impacts: most of them have recognizable ejecta blankets characterized by a radial ridge-and-trough pattern. The ring diameter ratios are often tantalizingly close to multiples of $\sqrt{2}$, although no one has yet suggested a convincing reason for this relationship.

Unlike the simple/complex and central peak/internal ring transitions discussed above, the transition from complex craters to multiring basins is not a simple function of g^{-1} . Although multiring basins are common on the Moon, where the smallest has a diameter of 410 km, none at all have been recognized on Mercury, with its 2 times larger gravity, even though the largest crater, Caloris basin, is 1300 km in diameter. The situation on Mars has been confused by erosion, but it is difficult to make a case that even the 1200 km diameter Argyre basin is a multiring structure. A very different type of multiring basin is found on Jupiter's satellite Callisto, where the 4000 km diameter Valhalla basin has dozens of closely-spaced rings that appear to face outward from the basin center. Another satellite of Jupiter, Ganymede, has both Valhalla-type and Orientale-type multiring structures. Since gravity evidently does not play a simple role in the complex crater/multiring basin transition, some other factor, such as the internal structure of the planet, may have to be invoked to explain the occurrence of multiring basins.

Aberrant Crater Types. On any planetary surface a few craters can always be found that do not fit the simple size-morphology relation described above. These are generally believed to be the results of unusual conditions of formation in either the impacting body or the planet struck. Circular craters with asymmetric ejecta blankets or elliptical craters with "butterfly-wing" ejecta patterns are the result of very low impact angles. Although moderately oblique impacts yield circular craters, at impact angles less than about 6° from the horizontal the final crater becomes elongated in the direction of flight. Small, apparently concentric, craters or craters with central dimples or mounds on their floors are the result of impact into a weak layer underlain by a stronger one. The ejecta blankets of some Martian craters show petal-like flow lobes that are believed to either indicate the presence of liquid water in the excavated material, or may be caused by ejecta interaction with atmospheric gasses. Some Venusian craters show extensive flow units in their ejecta whose origin is not currently well understood. Incorporation of dense atmospheric gasses or impact melt have been suggested as possibilities. Craters on Ganymede and Callisto develop central pits at a diameter where internal rings would be

expected on other bodies. The explanation for these pits is still unknown. Smaller craters on the Earth or Venus tend to form clusters of irregular craters, reflecting the effect of the atmosphere in breaking the original projectile into many smaller fragments before impact. In spite of these complications, however, the simple size-morphology relation described above provides a simple organizing principle into which most impact craters can be grouped.

Cratering Mechanics

The impact of an object moving at many km/sec on the surface of a planet initiates an orderly sequence of events that eventually produces an impact crater. Although this is really a continuous process, it is convenient to break it up into distinct stages that are each dominated by different physical processes. This division clarifies the description of the overall cratering process, but it should not be forgotten that the different stages really grade into one another and that a perfectly clean separation is not possible. The most commonly used division of the impact cratering process is into Contact and Compression, Excavation, and Modification.

Contact and Compression. Contact and compression is the briefest of the three stages, lasting only a few times longer than the time required for the impacting object (referred to hereafter as the "projectile") to traverse its own diameter, $\tau = L/v_i$, where τ is the duration of contact and compression, L is the projectile diameter, and v_i is the impact velocity. During this stage the projectile first contacts the planet's surface (hereafter, "target") and transfers its energy and momentum to the underlying rocks (Fig. 2). The specific kinetic energy (energy per unit mass, $1/2 v_i^2$) possessed by a projectile traveling at even a few km/sec is surprisingly large. A. C. Gifford, in 1924, first realized that the energy per unit mass of a body traveling at 3 km/sec is comparable to that of TNT. Gifford proposed the "impact-explosion analogy" which draws a close parallel between a high-speed impact and an explosion.

As the projectile plunges into the target, shock waves propagate both into the projectile, compressing and slowing it, and into the target, compressing and accelerating it downward and outward. At the interface between target and projectile the material of each moves at the same velocity. The shock wave in the projectile eventually reaches its back (or top) surface. At this time the pressure is released as the surface of the compressed projectile expands upward, and a wave of pressure relief propagates back downward toward the projectile-target interface. The contact and compression stage is considered to end when this relief wave reaches the projectile-target interface. At this

time the projectile has been compressed to high pressure, often reaching 100's of GPa, and upon decompression it may be in the liquid or gaseous state due to heat deposited in it during the irreversible compression process. The projectile generally carries off 50% or less of the total initial energy if the density and compressibility of the projectile and target material do not differ too much. The projectile-target interface at the end of contact and compression is generally less than a projectile diameter L below the original surface.

Contact and compression is accompanied by the formation of very high-velocity "jets" of highly shocked material. These jets form where strongly compressed material is close to a free surface, for example near the circle where a spherical projectile contacts a planar target. The jet velocity depends on the angle between the converging surface of the projectile and target, but may exceed the impact velocity by factors as great as 5. Jetting was initially regarded as a spectacular but not quantitatively important phenomenon in early impact experiments, where the incandescent streaks of jetted material only amounted to about 10% of the projectile's mass in vertical impacts. However, recent work on oblique impacts indicates that in this case jetting is much more important and that the entire projectile may participate in a downrange stream of debris that carries much of the original energy and momentum. Oblique impacts are still not well understood and more work needs to be done to clarify the role of jetting early in this process.

Excavation. During the excavation stage the shock wave created during contact and compression expands and eventually weakens into an elastic wave while the crater itself is opened by the much slower "excavation flow". The duration of this stage is roughly given by the period τ of a gravity wave (similar to a water wave in deep water in which the restoring force is gravity alone) with wavelength equal to the crater diameter D ; $\tau = (D/g)^{1/2}$, for craters whose excavation is dominated by gravity g (this includes craters larger than a few km in diameter, even when excavated in hard rock). Thus, Meteor Crater ($D = 1$ km) was excavated in about 10 seconds, while the 1000 km diameter Imbrium Basin on the Moon took about 13 minutes to open. Shock wave expansion and crater excavation, while intimately linked, occur at rather different rates and may be considered separately.

The high pressures attained during contact and compression are almost uniform over a volume roughly comparable to the initial dimensions of the projectile. However, as the shock wave expands away from the impact site the shock pressure declines as the initial impact energy spreads over an increasingly large volume of rock. The pressure in the shock P as a function of distance r from the impact site is given roughly by

$$P(r) = P_0 (a/r)^n$$

where $a (= L/2)$ is the radius of the projectile, P_0 is the pressure established during contact and compression, and the power n is between 2 and 4, depending on the strength of the shock wave (n is larger at higher pressures--a value $n=3$ is a good general average).

The shock wave, with a release wave immediately following, quickly attains the shape of a hemisphere expanding through the target rocks (Fig.3). The high shock pressures are confined to the surface of the hemisphere: the interior has already decompressed. The shock wave moves very quickly, as fast or faster than the speed of sound, between about 6 and 10 km/sec in most rocks. As rocks in the target are overrun by the shock waves, then released to low pressures, mineralogical changes take place in the component minerals. At the highest pressures the rocks may melt or even vaporize upon release. As the shock wave weakens, high pressure minerals such as coesite or stishovite arise from quartz in the target rocks, diamonds may be produced from graphite, or maskelynite from plagioclase. Somewhat lower pressures cause pervasive fracturing and "planar elements" in individual crystals. Still lower pressures create a characteristic cone-in-cone fracture called "shatter cones" (Fig. 4) that are readily recognized in the vicinity of impact structures. Indeed, many terrestrial impact structures were first recognized from the occurrence of shatter cones.

The expanding shock wave encounters a special condition near the free surface. The pressure at the surface must be zero at all times. Nevertheless, a short distance below the surface the pressure is essentially equal to P , defined above. This situation results in a thin layer of surface rocks being thrown upward at very high velocity (the theoretical maximum velocity approaches the impact speed v_i). Since the surface rocks are not compressed to high pressure, this results in the ejection of a small quantity of unshocked or lightly shocked rocks at speeds that may exceed the target planet's escape velocity. Although the total quantity of material ejected by this "spall" mechanism is probably only 1-3% of the total mass excavated from the crater, it is particularly important scientifically as this is probably the origin of the recently discovered meteorites from the Moon, and of the SNC (Shergottite, Nakhilite, and Chassignite) meteorites which are widely believed to have been ejected from Mars.

The weakening shock wave eventually degrades into elastic waves. These elastic waves are similar in many respects to the seismic waves produced by an earthquake, although impact-generated waves contain less of the destructive shear-wave energy than earthquake waves. The seismic waves produced by a large impact may have significant effects on the target planet, creating jumbled terrains at the antipode of the impact site. This effect has been observed opposite Caloris basin on Mercury and opposite Imbrium

and Orientale on the Moon. The equivalent Richter magnitude M caused by an impact of energy E ($=1/2 m_p v_i^2$) is given approximately by $M=0.67 \log_{10} E - 5.87$.

Target material engulfed by the shock wave is released a short time later. Upon release the material has a velocity that is only about 1/5 of the particle velocity in the shock wave. This "residual velocity" is due to thermodynamic irreversibility in the shock compression. It is this velocity field that eventually excavates the crater. The excavation velocity field has a characteristic downward-outward-then upward pattern (Fig. 5) that moves target material out of the crater, ejecting it at angles close to 45° at the rim. The streamlines of this flow cut across the contours of maximum shock pressure, so that material ejected at any time may contain material with a wide range of shock levels. Nevertheless, the early, fast ejecta generally contains a higher proportion of highly shocked material than the later, slower ejecta. Throughout its growth the crater is lined with highly shocked, often melted, target material.

The growing crater is at first hemispherical in shape. Its depth $H(t)$ and diameter $D(t)$ both grow approximately as $t^{0.4}$, where t is time after the impact. Hemispherical growth ceases after a time of about $(2H_t/g)^{1/2}$, where H_t is the final depth of the transient crater. At this time the crater depth stops increasing (it may even begin to decrease as collapse begins), but its diameter continues to increase. The crater shape thus becomes a shallow bowl, finally attaining a diameter roughly 3-4 times its depth. At this stage, before collapse modifies it, the crater is known as a "transient" crater. Even simple craters experience some collapse (which produces the breccia lens), so that the transient crater is always a brief intermediate stage in planetary crater formation. However, since most laboratory craters are "frozen" transient craters, much of our knowledge about crater dimensions refers to the transient stage only, and must be modified for application to planetary craters.

Laboratory, field, and computer studies of impact craters have all confirmed that only material lying above about 1/3 of the transient crater depth (or about 1/10 of the diameter) is thrown out of the crater. Material deeper than this is simply pushed downward into the target, where its volume is accommodated by deformation of the surrounding rocks. Thus, in sharp contrast to ejecta from volcanic craters, material in the ejecta blankets of impact craters does not sample the full depth of rock intersected by the crater.

The form of the transient crater produced during the excavation stage may be affected by such factors as obliquity of the impact (although the impact angle must be less than about 6° for a noticeably elliptical crater to form at impact velocities in excess of about 4 km/sec), the presence of a water table or layers of different strength, rock

structure, joints, or initial topography in the target. Each of these factors produces its own characteristic changes in the simple bowl-shaped transient crater form.

Modification. Shortly after the excavation flow opens the transient crater and the ejecta is launched onto ballistic trajectories, a major change takes place in the motion of debris within and beneath the crater. Instead of flowing upward and away from the crater center, the debris comes to a momentary halt, then begins to move downward and back toward the center whence it came. This collapse is generally attributed to gravity, although elastic rebound of the underlying, compressed rock layers may also play a role. The effects of collapse range from mere debris sliding and drainback in small craters to wholesale alteration of the form of larger craters in which the floors rise, central peaks appear, and the rims sink down into wide zones of stepped terraces. Great mountain rings or wide central pits may appear in still larger craters.

These different forms of crater collapse begin almost immediately after formation of the transient crater. The time scale of collapse is similar to that of excavation, occupying an interval of a few times $(D/g)^{1/2}$. Crater collapse and modification thus take place on time scales very much shorter than most geologic processes. The crater resulting from this collapse is then subject to the normal geologic processes of gradation, isostatic adjustment, infilling by lavas, etc. on geologic time scales. Such processes may eventually result in the obscuration or even total obliteration of the crater, depending on the planetary surface on which it forms.

The effects of collapse depend on the size of the crater. For transient craters smaller than about 15 km diameter on the Moon, or about 3 km on the Earth, modification entails only collapse of the relatively steep rim of the crater onto its floor. The resulting "simple crater" is a shallow bowl-shaped depression with a rim-to-rim diameter D about 5 times its depth below the rim H . In fresh craters the inner rim stands near the angle of repose, about 30° . Drilling in terrestrial craters shows that the crater floor is underlain by a lens of broken rock (mixed breccia) derived from all of the rock units intersected by the crater. The thickness of this breccia lens is typically $1/2$ the depth of the crater H . Volume conservation suggests that this collapse increases the original diameter of the crater by about 15%. The breccia lens often includes layers and lenses of highly shocked material mixed with much less-shocked country rock. A small volume of shocked or melted rock is often found at the bottom of the breccia lens.

Complex craters (Fig. 1 b, c) collapse more spectacularly. Walls slump, the floor is stratigraphically uplifted, central peaks or peak rings rise in the center and the floor is overlain by a thick layer of highly shocked impact melt. The detailed mechanism of collapse is still not fully understood because straightforward use of standard rock

mechanics models do not predict the type of collapse observed. The current best description of complex crater collapse utilizes a phenomenological strength model in which the material around the crater is approximated as a Bingham fluid, a material which responds elastically up to differential stresses of about 3 MPa, independent of overburden pressure, then flows as a viscous fluid with viscosity on the order of 1 GPa-sec at larger stresses. In a large collapsing crater the walls slump along discrete faults, forming terraces whose widths are controlled by the Bingham strength, and the floor rises, controlled by the viscosity, until the differential stresses fall below the 3 MPa strength limit. A central peak may rise, then collapse again in large craters, forming the observed internal ring (or rings). Fig. 6 illustrates this process schematically. The rock in the vicinity of a large impact may display such an unusual flow law because of the locally strong shaking driven by the large amount of seismic energy deposited by the impact.

The mechanics of the collapse that produces multiring basins (Fig. 1d) is even less well understood. Fig. 7 illustrates the structure of the Orientale Basin on the Moon with a highly vertically exaggerated cross section derived from both geological and geophysical data. Note the ring scarps are interpreted as inward-dipping faults above a pronounced mantle uplift beneath the basin's center. One idea that is currently gaining ground is that the ring scarps are normal faults that develop as the crust surrounding a large crater is pulled inward by the flow of underlying viscous mantle material toward the crater cavity (Fig. 8). An important aspect of this flow is that it must be confined in a low viscosity channel by more viscous material below, otherwise the flow simply uplifts the crater floor and radial faults, not ring scarps are the result. Special structural conditions are thus needed in the planet for multiring basins to form on its surface, so that a g^{-1} dependence for the transition from complex craters to multiring basins is not expected (or observed). This theory is capable of explaining both the lunar-type and Valhalla-type multiring basins as expressions of different lithosphere thickness.

Atmospheric Interactions. As fast-moving meteoroids enter the atmosphere of a planet, they are slowed by friction with the atmospheric gases and compressed by the deceleration. Small meteoroids are often vaporized by frictional heating and never reach the surface of the planet. Larger meteoroids are decelerated to terminal velocity and fall relatively gently to the surface of the planet. The diameter of a meteorite that loses 90% of its initial velocity in the atmosphere is given by $L = 0.15 P_{\text{surf}}/(\rho_p g_{\text{surf}} \sin \theta)$, where P_{surf} is the surface atmospheric pressure, ρ_p is the meteorite's density and g_{surf} is the planet's surface acceleration of gravity. L is typically about 1 m for Earth and 60 m for Venus. However, this equation assumes that the projectile reaches the surface intact,

whereas in fact aerodynamic stresses may crush all but the strongest meteorites. Once fractured, the fragments of an incoming meteorite travel slightly separate paths and strike the surface some distance apart from one another. This phenomenon gives rise to the widely-observed strewn fields of meteorites or craters on the Earth, which average roughly a kilometer or two in diameter. On Venus, clusters of small craters attributed to atmospheric breakup are spread over areas roughly 20 km in diameter [*Phillips et al.*, 1991].

The atmospheric blast wave and thermal radiation produced by an entering meteorite may also affect the surface: The 1908 explosion at Tunguska River, Siberia, was probably produced by the entry and dispersion of a 100 m diameter stony meteorite that leveled and scorched about 2000 km² of meter-diameter trees [*Chyba et al.*, 1993]. Radar-dark "sploches" up to 50 km in diameter on the surface of Venus are attributed to pulverization of surface rocks by strong blast waves from meteorites that were fragmented and dispersed in the dense atmosphere [*Zahnle*, 1992].

Other atmospheric interactions dominate the post-impact evolution of craters produced by meteorites sufficiently large to strike the surface with a large fraction of their initial energy. Vaporized projectile and target expand rapidly out of the resulting crater, forming a vapor plume that, if massive enough, may blow aside the surrounding atmosphere and accelerate to high speed. In the impacts of sufficiently large and fast projectiles some of this vapor plume material may even reach escape velocity and leave the planet, incidentally also removing some of the planet's atmosphere. Such "impact erosion" may have played a role in the early history of the Martian atmosphere [*Melosh and Vickery*, 1989]. In smaller impacts the vapor plume may temporarily blow aside the atmosphere, opening the way for widespread ballistic dispersal of melt droplets (tektites) above the atmosphere and permitting the formation of lunar-like ejection blankets even on planets with dense atmospheres, as has been observed on Venus.

Scaling of Crater Dimensions

One of the most frequently asked questions about an impact crater is "how big was the meteorite that made the crater?". Like many simple questions this has no simple answer. It should be obvious that the crater size depends upon the meteorite's speed, size and angle of entry. It also depends on such factors as the meteorite's composition, the material and composition of the target, surface gravity, presence or absence of an atmosphere, etc. The question of the original size of the meteorite is usually unanswerable because the speed and angle of impact are seldom known. The inverse question, of how large a crater will be produced by a given size meteorite with known

speed and incidence angle, is in principle much simpler to answer. However, even this prediction is uncertain because there is no observational or experimental data on the formative conditions of impact craters larger than a few tens of meters in diameter, while the impact structures of geologic interest range up to 1000 km in diameter. The traditional escape from this difficulty is to extrapolate beyond experimental knowledge by means of scaling laws.

The first scaling laws were introduced in 1950 by C. W. Lampson, who studied the craters produced by TNT explosions of different sizes. Lampson found that the craters were similar to one another if all dimensions (depth, diameter, depth of charge placement) were divided by the cube root of the explosive energy W . Thus, if the diameter D of a crater produced by an explosive energy W is wanted, it can be computed from the diameter D_0 of a crater produced by energy W_0 using the proportion:

$$D/D_0 = (W/W_0)^{1/3}$$

An exactly similar proportion may be written for the crater depth, H . This means that the ratio of depth to diameter, H/D , is independent of explosive energy W , a prediction that agrees reasonably well with observation. In more recent work on large explosions the exponent $1/3$ in this equation has been modified to $1/3.4$ to account for the effects of gravity on crater formation.

Although impacts and explosions have many similarities, a number of factors make them difficult to compare in detail. Thus, explosion craters are very sensitive to the charge's depth of burial. Although this quantity is well defined for explosions, there is no simple analog for impact craters. Similarly, the angle of impact has no analog for explosions. Nevertheless, energy-based scaling laws were very popular in the older impact literature, perhaps partly because nothing better existed, and many empirical schemes were devised to adapt the well-established explosion scaling laws to impacts.

This situation has changed radically in the last decade, however, thanks to more impact cratering experiments specifically designed to establish scaling laws. It has been shown that the great expansion of the crater during excavation tends to decouple the parameters describing the final crater from the parameters describing the projectile. If these sets of parameters are related by a single, dimensional "coupling parameter" (as seems to be the case) then it can be shown that crater parameters and projectile parameters are related by power-law scaling expressions with constant coefficients and exponents. Although this is a somewhat complex and rapidly-changing subject, the best current scaling relation for impact craters forming in competent rock (low porosity) targets whose growth is limited by gravity rather than target strength (i.e., all craters larger than a few km diameter) is given by

$$D_{at} = 1.8 \rho_p^{0.11} \rho_t^{-1/3} g^{-0.22} L^{0.13} W^{0.22} (\sin \theta)^{1/3}$$

where D_{at} is the diameter of the transient crater at the level of the original ground surface, ρ_p and ρ_t are densities of the projectile and target, respectively, g is surface gravity, L is projectile diameter, W is impact energy ($= \pi/12 L^3 \rho_p v_i^2$) and θ is the angle of impact from the vertical. All quantities are in SI units.

Crater depth H appears to be a constant times the diameter D_{at} . Although a few investigations have reported a weak velocity dependence for this ratio, the experimental situation is not yet clear.

The amount of melt and vapor produced in an impact obeys a rather different scaling law, since it is determined solely by the physics of shock wave expansion and not by the gravity field of the planet (at the time of melt formation the shock pressures far exceed gravitational pressures for all but planetary-size projectiles). A widely-used melt and vapor scaling law is:

$$\frac{\text{Mass of Melt}}{\text{Mass of Projectile}} = 0.14 \frac{v_i^2}{\epsilon_m} \quad \text{for } v_i \geq 12 \text{ km/s}$$

and

$$\frac{\text{Mass of Vapor}}{\text{Mass of Projectile}} = 0.4 \frac{v_i^2}{\epsilon_v} \quad \text{for } v_i \geq 35 \text{ km/s}$$

where $\epsilon_m = 3.4 \times 10^6$ J/Kg is the specific energy of melting and $\epsilon_v = 5.7 \times 10^7$ J/Kg is the specific energy of vaporization of silicate rocks.

Since the masses melted and vaporized are independent of surface gravity, while the transient crater diameter decreases as gravity increases, the relative volume of melt to material excavated increases with increasing crater diameter, as shown in Fig. 9. Very large craters may differ substantially in morphology from small ones because of this difference in relative melt volume. Similarly, craters of similar size on different planets (eg. lunar vs. terrestrial craters) may have substantially different relative volumes of impact melt.

Impacts and Planetary Evolution

Modern theories of planetary origin suggest that the planets and the sun formed simultaneously 4.6×10^9 years ago from a dusty, hydrogen-rich nebula. Nebular condensation and hydrodynamic interactions were probably only capable of producing ca. 10 km diameter "planetesimals" that accreted into planetary scale objects by means of collisions. The time scale for accretion of the inner planets by mutual collisions is

currently believed to be between a few tens and one hundred million years. Initially rather gentle, these collisions became more violent as the random velocities of the smaller planetesimals increased during close approaches to the larger bodies. The mean random velocity of a swarm of planetesimals is comparable to the escape velocity of the largest object, so as the growing planetary embryos reached lunar size collisions began to occur at several kilometers per second. At such speeds impacts among the smaller objects were disruptive, whereas the larger objects had sufficient gravitational binding energy to accrete most of the material which struck them. Infalling planetesimals bring not only mass, but also heat to the growing planets. In the past it was believed that the temperature inside a growing planet increased in a regular way from near zero at the center to large values at the outside, reflecting the increase in collision velocity as the planet became more massive. However, it now seems probably that the size distribution of the planetesimal population was more evenly graded between large and small objects, and that each growing planetary embryo was subjected to many collisions with bodies up to 10% of the mass of the embryo itself. Such catastrophic collisions deposit heat deep within the core of the impacted body, wiping out any regular law for temperature increase with increasing radius and making the thermal evolution of growing planets rather stochastic [*Melosh, 1990*].

The origin of the Moon is now attributed to a collision between the proto-earth and a Mars-size protoplanet near the end of accretion 4.5×10^9 years ago. This theory has recently supplanted the three classic theories of lunar origin (capture, fission, and co-accretion) because only the giant impact theory provides a simple explanation for the Moon's chemistry, as revealed in the lunar rocks returned by Apollo. One view of this process is that a grazing collision vaporized (by jetting) a large quantity of the proto-Earth's mantle along with a comparable quantity of the projectile. While most of the mass of the projectile merged with the Earth (incidentally strongly heating the Earth: If the Earth was not molten before this impact it almost certainly was afterward), one or two lunar masses of vapor condensed into dust in stable Keplerian orbits about the Earth and then later accumulated together to form the Moon.

Sometime after the Moon formed and before about 3.8×10^9 years ago the inner planets and their satellites were subjected to the "late heavy bombardment", an era during which the cratering flux was orders of magnitude larger than at present. The crater scars of this period are preserved in the lunar highlands and the most ancient terrains of Mars and Mercury. A fit to the lunar crater densities using age data from Apollo samples [*Melosh and Vickery, 1989*] gives a cumulative crater density through geologic time of

$$N_{\text{cum}}(D>4 \text{ km}) = 2.68 \times 10^{-5} [T + 4.57 \times 10^{-7} (e^{\lambda T} - 1)]$$

Where $N_{\text{cum}}(D>4 \text{ km})$ is the cumulative crater density (craters/km²) of craters larger than 4 km diameter, T is the age of the surface in Gyr ($T=0$ is the present) and $\lambda=4.53 \text{ Gyr}^{-1}$. Several other slightly different fits to the same data have been discussed in the literature. The current cratering rate on the moon is about 2.7×10^{-14} craters with $D>4 \text{ km/km}^2/\text{yr}$. On the Earth the cratering rate has been estimated to be about 1.8×10^{-15} craters with $D>22.6 \text{ km/km}^2/\text{yr}$, which is comparable to the lunar flux taking into account the different minimum sizes, since the cumulative number of craters $N_{\text{cum}}(D) \sim D^{1.8}$. There is currently much debate about these cratering rates, which might be uncertain by as much as a factor of 2.

The study of relative crater densities (number per unit area) on planetary surfaces provides an important tool for establishing relative ages of surface features. Since impacts are generally presumed to occur randomly on a surface (a minor exception is the leading-trailing edge cratering rate asymmetry on the tidally-locked satellites of the giant planets), the spatial distribution of craters provides no information. However, older surfaces have been struck by more impacts than younger surfaces, so that crater density is a useful indicator of relative age on a given planet or satellite. Absolute ages require calibration of the cratering rate as a function of time, which generally requires radiometric dating of surfaces of known crater density. Such information is currently available only for the Moon. Similarly, interplanetary correlations of crater density are difficult because the cratering rate may differ in different parts of the solar system. A limitation of the relative crater density technique is that once the crater density becomes high enough, the addition of a new crater of some size wipes out, on average, an old crater of the same size (not to mention many smaller ones). A surface reaching this condition is in equilibrium (sometimes the word "saturation" is used interchangeably), and provides no age information subsequent to the time that equilibrium was achieved. The lunar highlands are widely believed to have reached this state.

The high cratering rates in the past indicate that the ancient Earth should have been heavily scarred by large impacts. Based on the lunar record it is estimated that more than 100 impact craters with diameters greater than 1000 km should have formed on the Earth. Although little evidence of these early craters has yet been found, it is gratifying to note the recent discovery of thick impact ejecta deposits in 3.2 to 3.5 Gyr Archean greenstone belts in both South Africa and Western Australia. Since rocks have recently been found dating back to 4.2 Gyr, well into the era of heavy bombardment, it is to be hoped that more evidence for early large craters will be eventually discovered. Heavy

bombardment also seems to have overlapped the origin of life on Earth. It is possible that impacts may have had an influence on the origin of life, although whether they suppressed it by creating global climatic catastrophes (up to evaporation of part or all of the seas by large impacts), or facilitated it by bringing in needed organic precursor molecules, is unclear at present. The relation between impacts and the origin of life is currently an area of vigorous speculation.

The idea that large impacts can induce major volcanic eruptions is a recurring theme in the geologic literature. This idea probably derives from the observation that all of the large impact basins on the Moon's nearside are flooded with basalt. However, radiometric dates on Apollo samples made it clear that the lava infillings of the lunar basins are nearly 1 Gyr younger than the basins themselves. Furthermore, the farside lunar basins generally lack any substantial lava fill. The nearside basins are apparently flooded merely because they were topographic lows in a region of thin crust at the time that mare basalts were produced in the Moon's upper mantle. Simple estimates of the pressure release caused by stratigraphic uplift beneath large impact craters makes it clear that pressure release melting cannot be important in impacts unless the underlying mantle is near the melting point before the impact. Thus, to date, there is no firm evidence that impacts can induce volcanic activity. Impact craters may create fractures along with preexisting magma may escape, but themselves are probably not capable of producing much melt. The massive igneous body associated with the Sudbury, Ontario impact structure is now attributed to a thick impact melt sheet [*Grieve et al.*, 1991], rather than to impact-induced intrusive activity.

The most recent major impact event on Earth seems to have been a collision between the Earth and a 10 km diameter comet or asteroid 65 Myr ago that ended the Cretaceous era and caused the most massive biological extinction in recent geologic history. Evidence for this impact has been gathered from many sites over the last decade, and now seems nearly incontrovertible. First detected in an enrichment of the siderophile element iridium in the ca. 3 mm thick K/T (Cretaceous/Tertiary) boundary layer in Gubbio, Italy, the iridium signature has now been found in more than 100 locations worldwide, in both marine and terrestrial deposits. Accompanying this iridium are other siderophile elements in chondritic ratios, shocked quartz grains, coesite, stishovite and small (100-500 μ) spherules resembling microtektites. All these point to the occurrence of a major impact at the K/T boundary. In addition, soot and charcoal have been found at a number of widely-separated sites in abundances that suggest that the entire world's standing biomass burned within a short time of the impact. An impact of this magnitude should have produced a crater nearly 200 km in diameter. A very strong candidate for

this crater has been found beneath the cover rocks of the Northern Yucatan Peninsula. Named Chicxulub Crater by its discoverer, Glen Penfield [*Hildebrand et al.*1991], it is about 180 km in diameter. Although many details of the impact, and especially of the extinction mechanism, still have to be worked out, the evidence for a great impact at this time has becoming overwhelming, although a few geologists still adhere to some kind of volcanically-induced extinction crisis. Future work should be able to resolve the mysteries surrounding this striking demonstration of the importance of impact craters in both solar system and Earth history.

H. J. MELOSH

References

Nearly all of the material summarized in this article can be found explained at greater length, with original references in:

H. J. Melosh, *Impact Cratering: A Geologic Process*, Oxford University Press, 1989, 245pp.

References to article which appeared after 1989:

Chyba, C. F., P. J. Thomas, and K. J. Zahnle, Atmospheric disruption of small comets and asteroids and the 1908 Tunguska explosion, *Nature*, 361, 40-44, 1993.

Grieve, R. A. F., D. Stöffler, and A. Deutsch, The Sudbury Structure: Controversial or Misunderstood?, *J. Geophys. Res.*, 96, 22,753-22,764, 1991.

Hildebrand, A. R., G. T. Penfield, D. A. Kring, M. Pilkington, A. Camargo Z., S. B. Jacobsen, and W. V. Boynton, Chicxulub Crater: A possible Cretaceous/Tertiary boundary impact crater on the Yucatán Peninsula, Mexico, *Geology*, 19, 867-871, 1991.

Melosh, H. J., Giant impacts and the thermal state of the early Earth, in *Origin of the Earth*, edited by J. H. Jones, and H. E. Newsom, pp. 69-83, Oxford University Press, New York, 1990.

Melosh, H. J., and A. M. Vickery, Impact erosion of the primordial atmosphere of Mars, *Nature*, 338, 487-489, 1989.

Phillips, R. J., R. E. Arvidson, J. M. Boyce, D. B. Campbell, J. E. Guest, G. G. Schaber, and L. A. Soderblom, Impact craters on Venus: Initial analysis from Magellan, *Science*, 252, 288-297, 1991.

Zahnle, K. J., Airburst origin of dark shadows on Venus, *J. Geophys. Res.*, 97, 10,243-10,255, 1992.

Figure Captions:

Fig. 1 Impact crater morphology as a function of increasing size. (a) Simple crater: 2.5 km diameter crater Linné in western Mare Serenitatis on the Moon (Apollo 15 Panametric Photo strip 9353), (b) Complex crater with central peak: 102 km diameter crater Theophilus on the Moon (Apollo 16 Hasselblad photo 0692). (c) Complex crater with internal ring: Mercurian craters Strindberg (165 km diameter) to the lower left and Ahmad Baba (115 km) to the upper right (Mariner 10 FDS 150, rectified). (d) Multiring basin: 620 km diameter (of most prominent ring) Orientale basin on the Moon (Lunar Orbiter IV medium resolution frame 194).

Fig. 2 Three frames (a-c) showing the evolution of shock waves in the contact and compression stage of the vertical impact of a 46.4 km diameter iron projectile on a gabbroic anorthosite target at 15 km/s. The last frame (d) is a very early phase of the excavation stage. Pressure contours are given in GPa, and the times are given in units of τ , defined in the text. Note the change in lengths of the scale bar from frame to frame.

Fig. 3 Schematic illustration of the expanding shock wave and excavation flow following a meteorite impact. The contours in the upper part of the figure represent pressure at some particular time after the impact. The region of high shock pressure is seen to be isolated or "detached" on an expanding hemispherical shell. The insets show profiles of particle velocity and pressure along the section AA'. The dashed lines on these insets show particle velocity and pressure some time later than those shown by the solid lines, and the solid curves connecting the peaks are portions of the "envelopes" of peak particle velocity and peak pressure.

Fig. 4 Shatter cones from the Spider Structure, W. Australia, formed in mid-Proterozoic orthoquartzite. This cone-in-cone fracture is characteristic of shattering by impact-generated shock waves. The scale bar on top is 15 cm long. Courtesy of George Williams.

Fig. 5 Geometry of the excavation flow field which develops behind the rapidly expanding shock front, which has moved beyond the boundaries of this illustration. The lines with arrows indicate "stream tubes" along which material flows downward and outward from the crater. The stream tubes cut across the contours of maximum shock

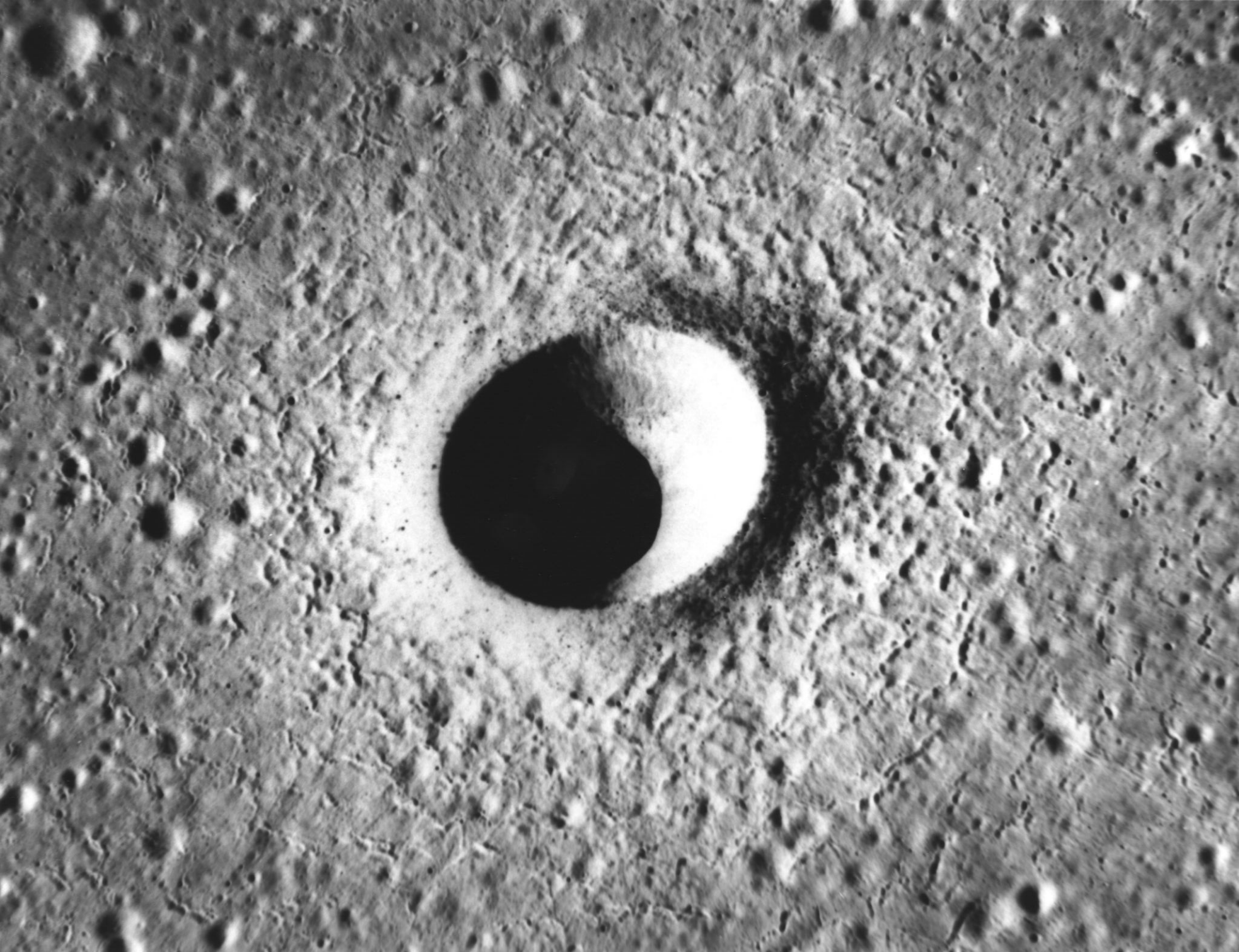
pressure, showing that material ejected at any given range from the impact site has been shocked to a variety of different maximum pressures. When material flowing through a streamtube crosses the initial surface it forms part of the ejecta curtain. Ejecta emerging near the impact site travels at high speed, whereas ejecta emerging at larger distances travels at slower velocities.

Fig. 6 Schematic illustration of the formation of complex craters with either (a) central peaks or (b) peak rings. Uplift of the crater begins even before the rim is fully formed. As the floor rises further, rim collapse creates a wreath of terraces surrounding the crater. In smaller craters the central uplift "freezes" to form a central peak. In larger craters the central peak collapses and creates a peak ring before motion ceases.

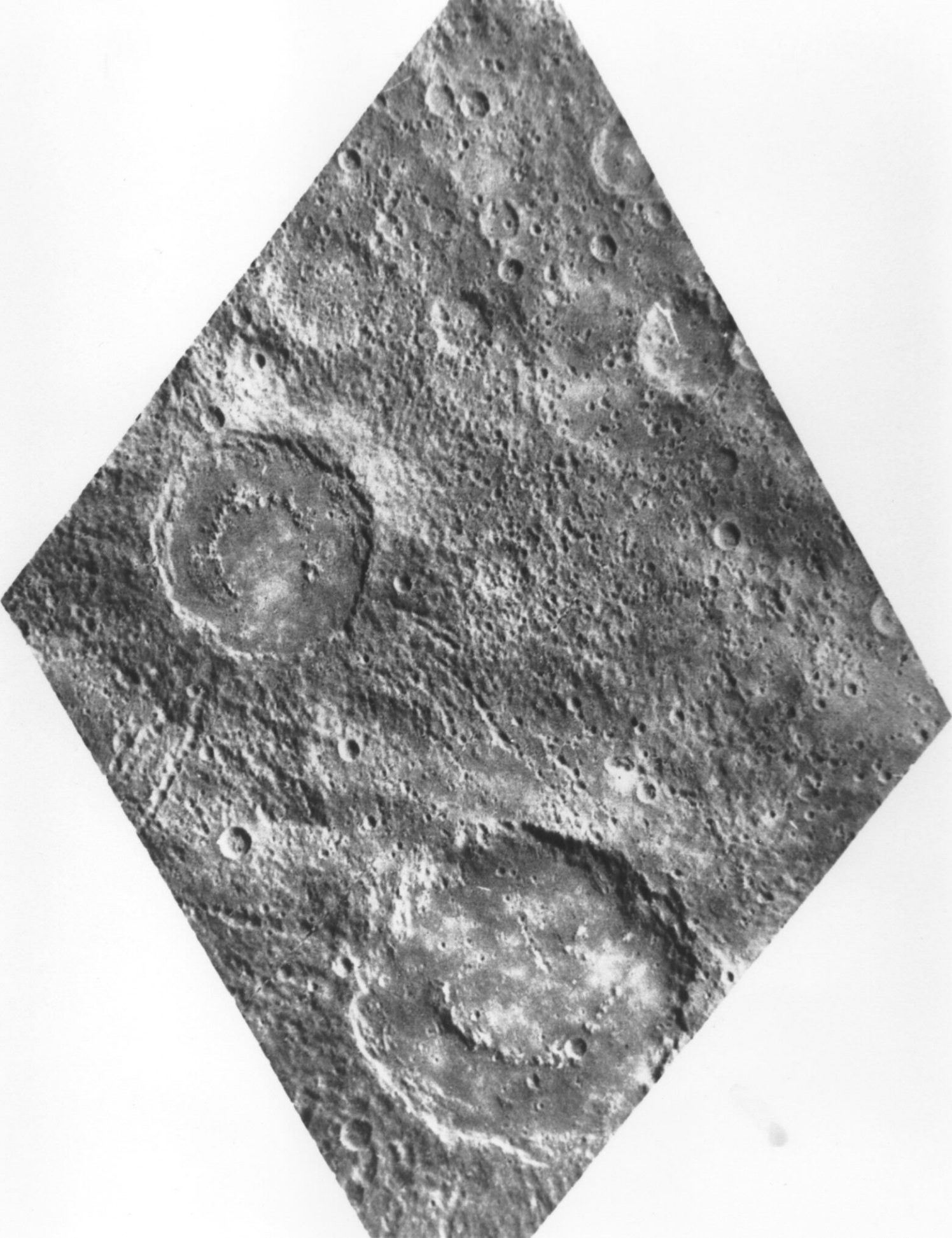
Fig. 7 Geologic and geophysical structure of the Orientale Basin on the Moon, one of the freshest and best studied multiring basin. A dense mantle plug underlies the center of the basin. The crustal thinning above the plug is due to the ejection of about 40 km of crustal material from the crater that formed the basin. The great ring scarps shown in cross section formed during collapse of the crater. Note the 10X vertical exaggeration necessary to show the ring scarps.

Fig. 8 The ring tectonic theory of multiring basin formation. (a) shows the formation of a normal complex crater in a planet with uniform rheology. (b) shows the inward-directed flow in a more fluid asthenosphere underlying a lithosphere of thickness comparable to the crater depth and the resulting scarps. (c) shows a Valhalla-type basin developing around a crater formed in very thin lithosphere.

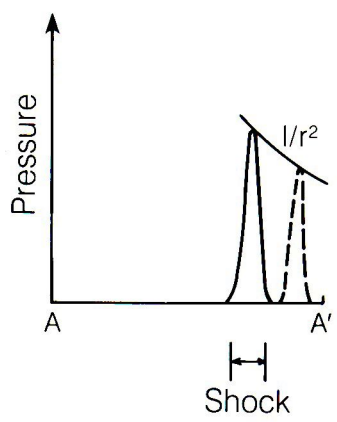
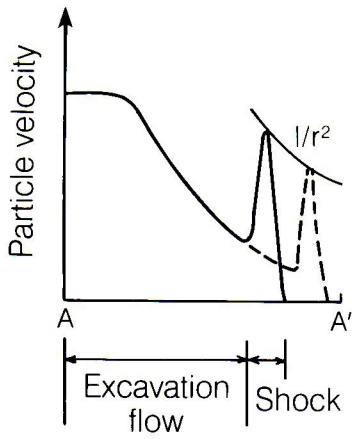
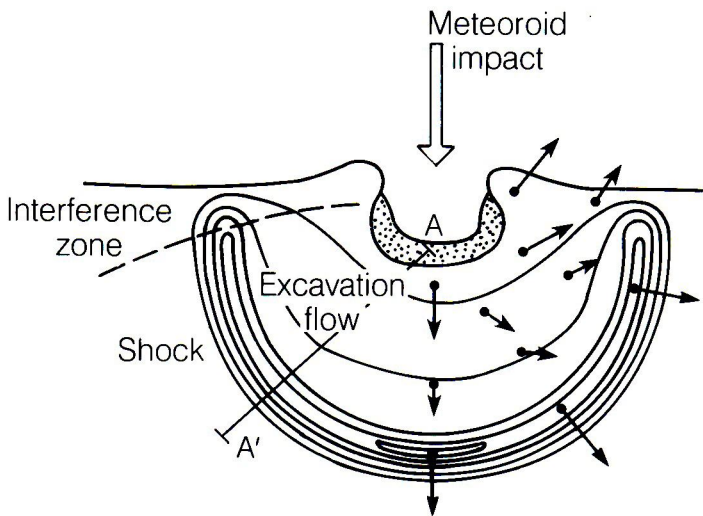
Fig. 9 The different scaling laws for crater diameter and melt or vapor volume imply that as the crater diameter increases the volume of melted or vaporized material may approach the volume of the crater itself. This figure is constructed for impacts at 35 km/s on the Earth.

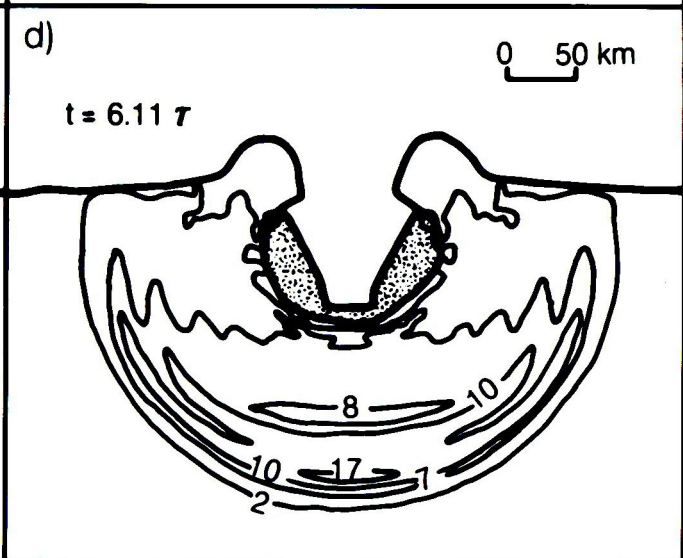
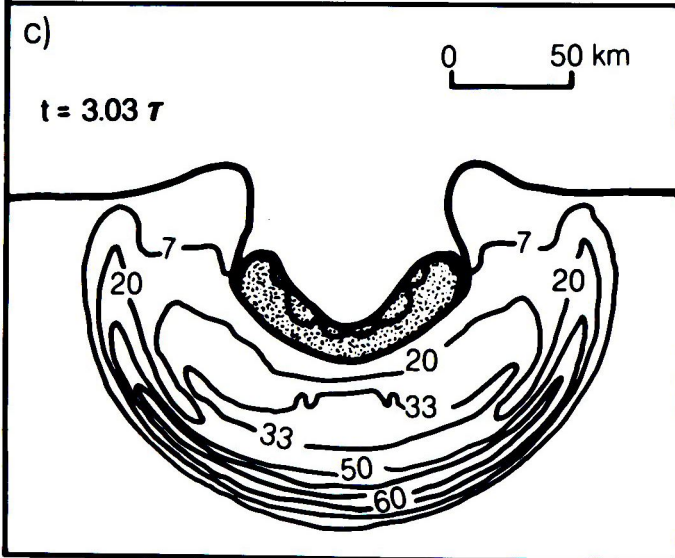
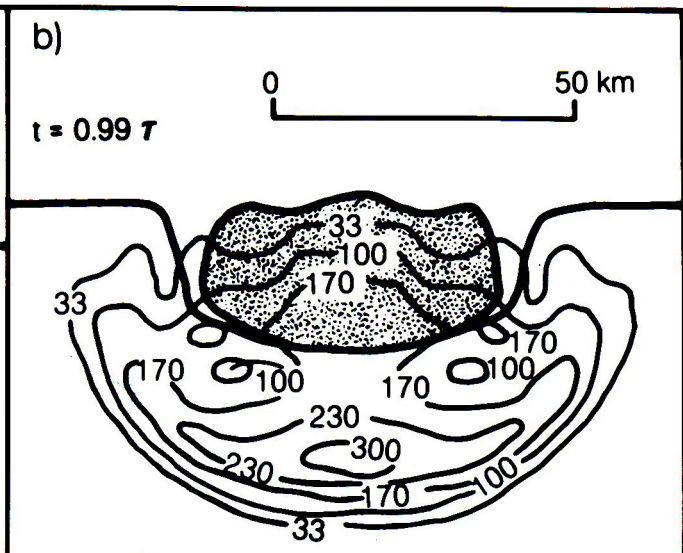
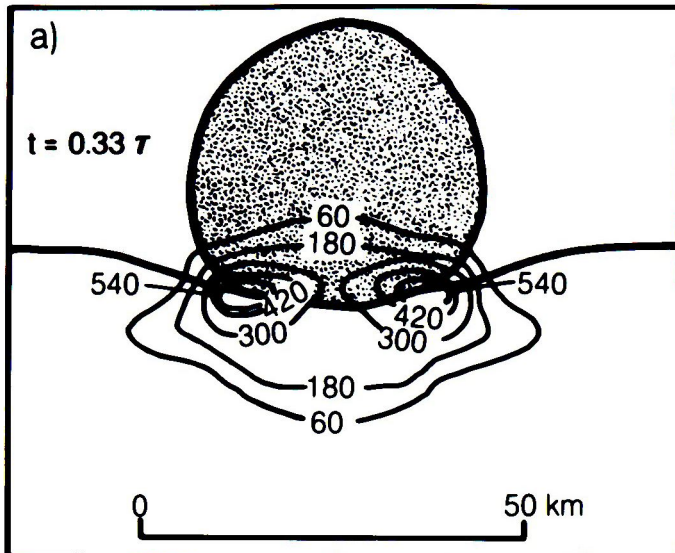




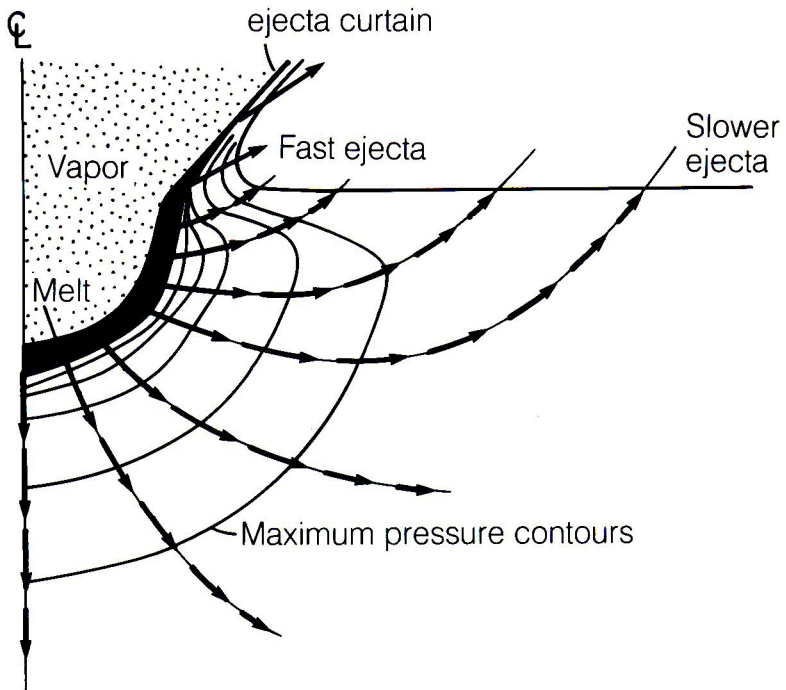




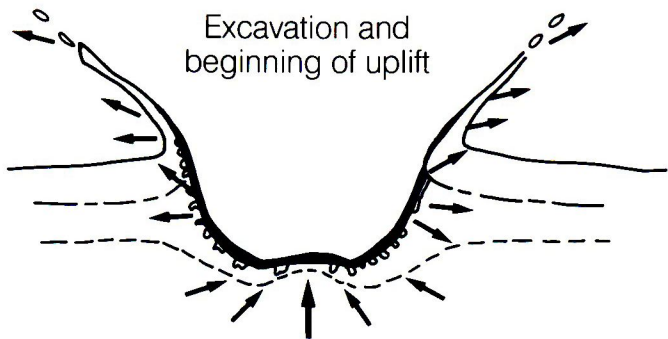




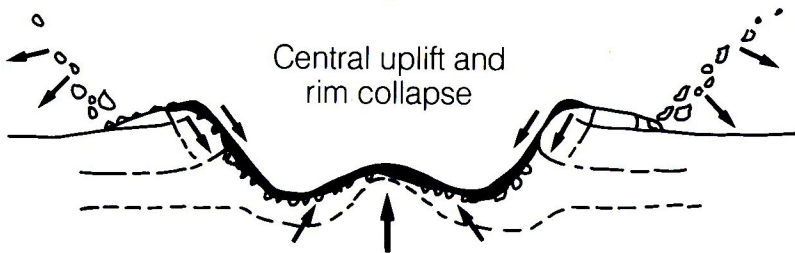




Excavation and
beginning of uplift



Central uplift and
rim collapse

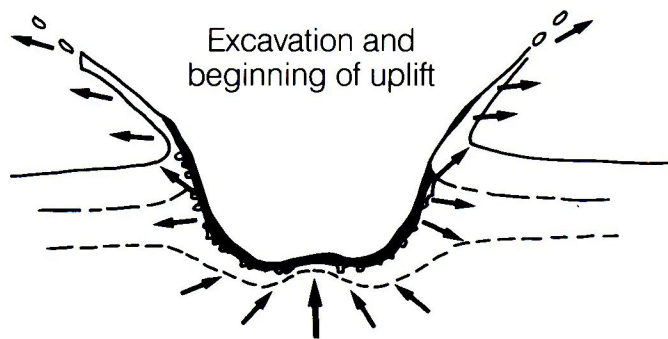


Final crater

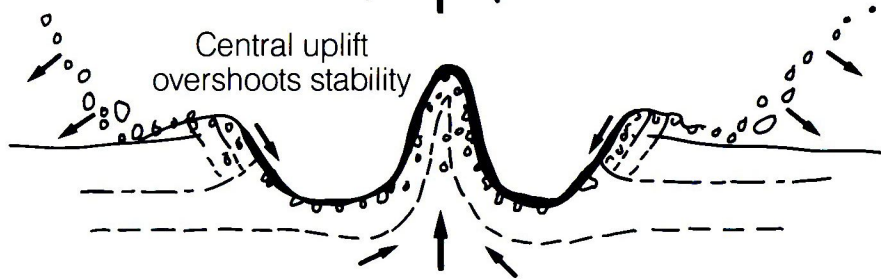


(a)

Excavation and
beginning of uplift



Central uplift
overshoots stability

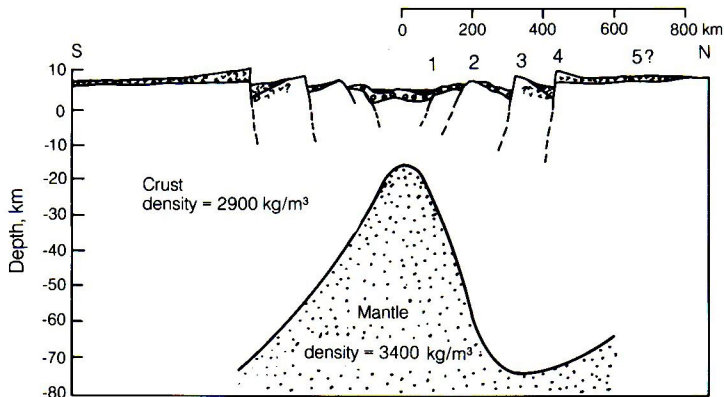



Peak ring crater



(b)

- 1 - Inner basin ring
- 2 - Inner rock
- 3 - Rook
- 4 - Cordillera
- 5 - Questionable ring



 Prebasin rocks
(highly brecciated
toward basin
center)

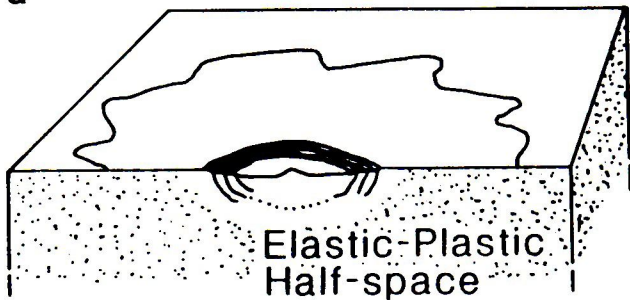
 Hevelius
formation
(ejecta)

 Rock
material
(slumps?)

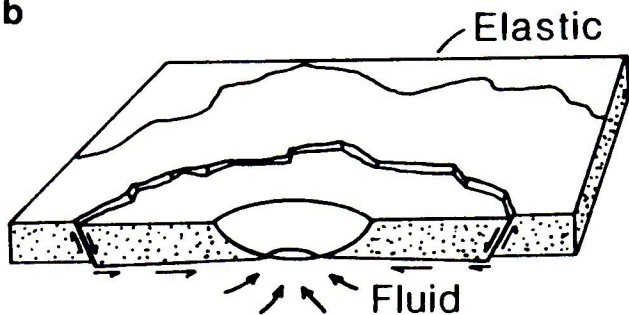
 Cracked
floor material
(impact melt?)

 Mare
basalt

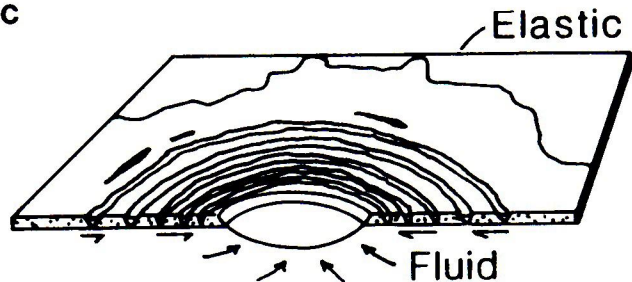
a



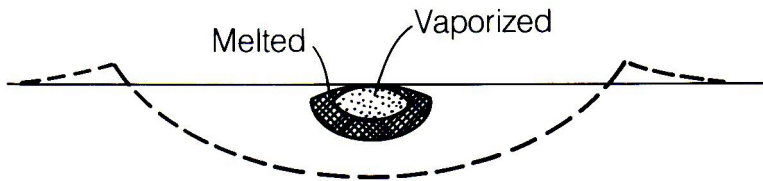
b



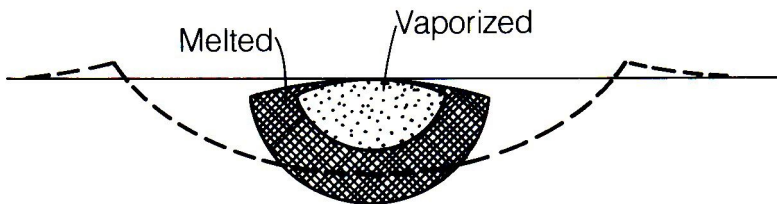
c



$D_{at} = 10\text{km}$



$D_{at} = 100\text{km}$



$D_{at} = 1000\text{km}$

